Control strategy and optimization of the indoor ski simulator

Hao Shi *, Zhen Chen, Ning Dong, Qing Fei, Xiaolan Yao, Wanshuai Hu

School of Automation, Beijing Institute of Technology
5 Zhongguancun South Street, Haidian District, Beijing 100081, P.R.China
E-mail: 865459245@qq.com

Abstract. This paper is based on a self-developed indoor ski simulator for ski training and entertainment, which can simulate slalom and combine it with virtual scenes to allow skiers to have a more realistic skiing experience. Firstly, the model of the skiing movement is analyzed, and the nonlinear control strategy of the motor velocity of the ski simulator is proposed. For the relative lag between the virtual scenes and the current skier's position, we use a neural network to make predictions and use a sparrow search algorithm (SSA) to optimize neural network weights and thresholds. The simulation and experimental results indicate that this method can effectively predict.

Keywords: Simulated ski platform, Nonlinear function, Neural network, Sparrow search algorithm

1. INTRODUCTION

The successful hosting of the 24th Winter Olympics Games has greatly promoted the development of China's ski industry. Ski sports gradually moved from the niche to the public and from the north to the whole country, it becomes a sports and entertainment activity loved by the whole people. However, skiing has high requirements on venues and seasons, so indoor ski simulators are essential to further promote this sport and let more people participate in this sport.

The current mainstream indoor ski simulators are as follows: The first kind of simulator has a simple structure and is only realized by visual or platform vibration, which is used for simple entertainment[1]. The second is a sliding carpet simulator, which can meet the needs of skiers by simulating skiing on the slope[2]. The third is multi-degree-of-freedom simulated skiing equipment, Beijing Jiaotong University realized the indoor ski simulator using the 3-DOF parallel mechanism platform[3]. The equipment has done preliminary research on the 3-DOF platform and virtual reality.

This paper is based on the indoor ski simulator independently developed by the research group. Through the modeling and analysis of alpine skiing actions, we can obtain the relationship between the motor velocity and the vertical edge angle and then design the nonlinear control algorithm for the motor velocity of the platform. During the actual operation, we found that there is a relative lag between the animation effect of the virtual interface and the current location of the skier due to the communication delay. We use BP neural network to make predictions about the skier's location. To make the prediction results of the neural network more accurate, the sparrow search algorithm is used to optimize the parameters of the neural network. Enhanced the simulated skiing effect of the simulator, making skiers feel like they are skiing.

2. ANALYSIS OF SKI SPORTS MODEL

Downhill and slalom are the two most basic and important skills in alpine skiing competitions. This section mainly models and analysis these two skiing sports, which provides a basis for the design of the indoor ski simulator.

2.1. Downhill model analysis

Downhill is a sport that uses gravity to quickly slide down a mountain[4]. During the competition, the athlete adjusts the skis to be parallel and shoulder-width apart. At this time, the weight of the skier is mainly supported by the soles of the two feet. The feet step on the skis to make the skis evenly stressed. The center of gravity will sink slightly and move forward. In the process, the skier can slide down only by the skier's gravity. The downhill model is shown in Fig.1.

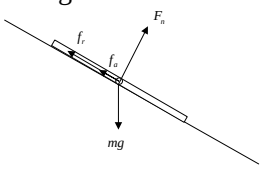


Fig.1. Downhill model

When the system is in equilibrium there are:

$$\begin{aligned} mg\sin\alpha-(f_a+f_r)=0 \\ F_n-mg\cos\alpha=0 \end{aligned} \tag{1}$$

Where f_a is the air drag force, f_r is the friction, and F_n is the reaction force of snow surface, α is the slope of the terrain.

Air drag force[5] f_a is:

$$f_a=-\frac{C_d\rho_a A}{2}sign(v)v^2 \tag{2}$$

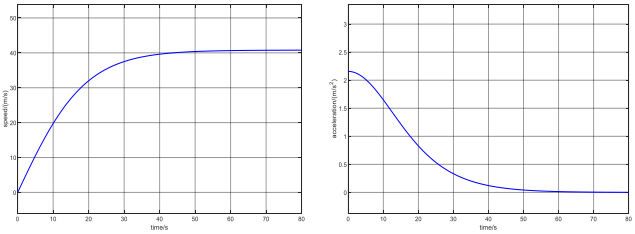
Where ρ_a is the air density, C_d is the air drag coefficient, A is the frontal area of the body in the airflow, and v is the velocity of the skier.

Friction f_r is:

$$f_r = \mu F_n \tag{3}$$

Where μ is the dynamic friction factor of snow.

A flat ski track with a slope of 15° is used for the downhill model analysis. The skier's weight is set to 70kg, the height is set to 1.7m and the air drag coefficient is set to 0.45. After simulation analysis, the skier's downhill velocity and acceleration are shown in Fig.2.



(a)velocity (b) acceleration

Fig.2: Downhill simulation results

According to the simulation results of the downhill model, when the skier is downhill, the acceleration of the skier will gradually reduce and the speed of the skier will gradually arrive at the maximum. The downhill velocity is mainly related to the skier's weight and the ski field factors during skiing, such as speed of the wind, slope, quality of snow, etc.

2.2. Slalom model analysis

In the alpine skiing slalom event, the skier relies on the body to drive the snowboard when turning. Firstly, the skier controls the inclination of the upper body to overcome the inertance of the body's backward leaning. And then drives the snowboard to incline through the lower limbs, so that the skier can complete the slalom. The board is at the optimum angle, shortening the taxi time. The ski slalom model is shown in Fig.3.

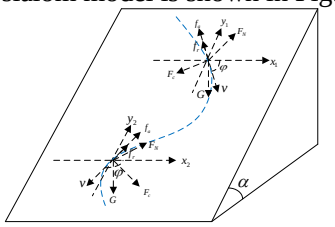


Fig.3 Slalom model

The Cartesian coordinate system is established on the slope and the model is subjected to force analysis through Newton's second law. Breaking it down into x_1Oy_1 and x_2Oy_2 coordinate systems respectively and merging it later:

$$\begin{aligned} ma_x &= -F_c \sin\varphi \operatorname{sgn}\dot{\varphi} - (f_a + f_r)\cos\varphi \\ ma_y &= G\sin\alpha + F_c \sin\varphi \operatorname{sgn}\dot{\varphi} - (f_a + f_r)\cos\varphi \end{aligned} \tag{4}$$

Then we use Newton's second law in the tangential and radial directions:

$$\begin{aligned} m\dot{v} &= G'\cos\varphi - (f_a + f_r) \\ \frac{mv^2}{R_c} &= F_c + G'\cos\varphi \operatorname{sgn}\dot{\varphi} \end{aligned} \tag{5}$$

Where $R_c = R\cdot\cos\theta$, R_c is the local radius of curvature of the trajectory, R is side cut radius of the ski, and θ is the edge angle.

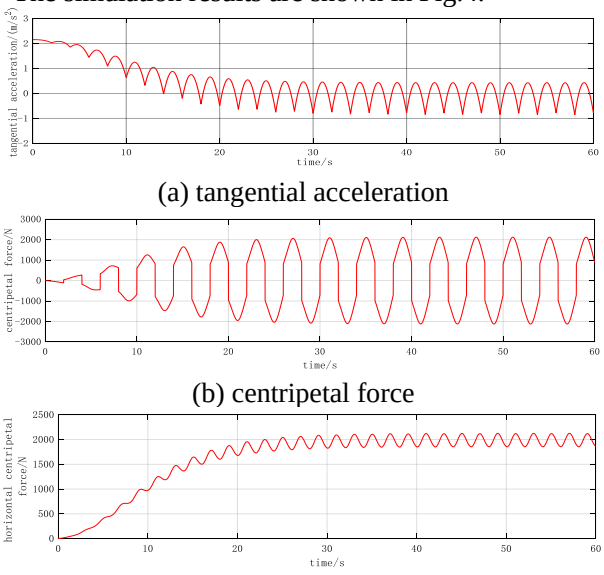
According to the principle of kinematics, we can get:

$$\begin{aligned} a_x &= (v\sin\varphi)' = \dot{v}\sin\varphi + v\dot{\varphi}\cos\varphi \\ a_y &= (v\cos\varphi)' = \dot{v}\cos\varphi - v\dot{\varphi}\sin\varphi \end{aligned} \tag{6}$$

Combining the above equations can be obtained:

$$\begin{cases} \dot{\varphi} = \dfrac{v}{R_c}\operatorname{sgn}\dot{\varphi} \\ \dot{v} = g\sin\alpha\sin\varphi - \mu g\cos\alpha - \dfrac{C_d\rho_a A}{2m}v^2 \end{cases} \tag{7}$$

The simulation results are shown in Fig.4.



(a) tangential acceleration

(b) centripetal force

(c) horizontal centripetal force

Fig.4 Slalom simulation results

3. INDOOR SKI SIMULATOR VELOCITY CONTROL STRATEGY

3.1. Modeling and analysis of slalom velocity

During the slalom model[6], the force condition of the skier is shown in Fig.5.



Fig.5 Force analysis of slalom motion

Where θ is the edge angle, G is the skier's gravity, f_s is the component of gravity perpendicular to the ground, f_t is the gravity component in the direction of the velocity, and f_b is the radial resultant force that provides the centripetal force.

$$\begin{aligned} F_N &= f_s = mg\cos\alpha \\ f_t &= mg\sin\alpha - f_a - f_r \\ \tan\theta &= \frac{F}{F_N} = \frac{f_b}{f_s} \end{aligned} \tag{8}$$

Where α is the slope of the terrain, F is the rotary centripetal force.

According to the force analysis of slalom motion, it can be seen that the lateral crural is mainly used to provide the centripetal force required for the ski turn. According to the

above analysis, the pulling force that the motor needs to provide is:

$$F = mg \cdot \cos\alpha \cdot \tan\theta \tag{9}$$

It can be seen from the above formula that under the condition of a certain slope, the pulling force of the motor is related to the edge angle.

3.2. Introduction of the indoor ski simulator

The indoor ski simulator can simulate the slalom in alpine skiing by driving the skier to move laterally on the slideway. To ensure a more realistic simulated skiing experience and improve stability, the indoor ski simulator is powered by four motors. The four motors are respectively fixed at both ends of the platform with rope drive wheels. The wire rope is wound on the rope drive wheels and connected to the skis. The skis are driven to slide on the slideway by the rotation of the motor.

Attitude sensors are installed inside the ski, which can detect the inclination angle of the ski, that is, the edge angle. Laser sensors are attached to both sides of the slideway, which can detect the current position of the ski on the slideway. When the controller receives the change of the inclination angle of the ski, it will control the motor to rotate and drive the ski to slide left and right on the slideway through the wire rope. And the speed of the motor is also associated with the ratio of change of the edge angle. When the edge angle changes faster, the motor velocity will rise or drop rapidly accordingly.

Safety gratings are attached to both sides of the slideway to make sure the safety of skiers. When there is an obstacle on the slideway or the skier falls, the indoor ski simulator stops immediately.

3.3. Nonlinear Control Algorithm for Motor velocity

In this thesis, we adopt the nonlinear *fal* function control algorithm in the active disturbance rejection control algorithm[7]. By optimizing it and regulating the proportional parameters, the motor can be controlled smoothly.

fal function is a special nonlinear structure in the control field. It is a mathematical fitting of the experience of the control engineering community[8]. It has the characteristics of rapid convergence and has become a commonly used non-linear structure. In this paper, the *fal* function is transformed into a continuous smooth curve in the whole real number domain to improve its performance and the stability of motor control.

fal function expression is:

$$fal(e,\alpha,\delta) = \begin{cases} |e|^{\alpha} sign(e) & |e| > \delta \\ \dfrac{e}{\delta^{1-\alpha}} & |e| \le \delta \end{cases} \tag{10}$$

In the interval $|e| > \delta$, it is the same as the original function. In the interval $|e| \le \delta$, to make sure that the function after transformation is 0 and continuous at the origin, The *fal* function selection is as follows:

$$fal(e,\alpha,\delta) = xe^3 + ye^2 + ze \tag{11}$$

Assuming the function is continuously differentiable, then at the piecewise point:

$$\begin{aligned} \lim_{e\to\pm\delta^-} fal(e,\alpha,\delta) &= \lim_{e\to\pm\delta^+} fal(e,\alpha,\delta) = \lim_{e\to\pm\delta} fal(e,\alpha,\delta) \\ \lim_{e\to\pm\delta^-} fal'(e,\alpha,\delta) &= \lim_{e\to\pm\delta^+} fal'(e,\alpha,\delta) = \lim_{e\to\pm\delta} fal'(e,\alpha,\delta) \end{aligned} \tag{12}$$

And the *fal* function should also be differentiable at the origin:

$$\lim_{e=0} fal'(e,\alpha,\delta) = \frac{|\delta|^{\alpha} sign(\delta) - |-\delta|^{\alpha} sign(-\delta)}{2\delta} \tag{13}$$

Obtained from the above formula:

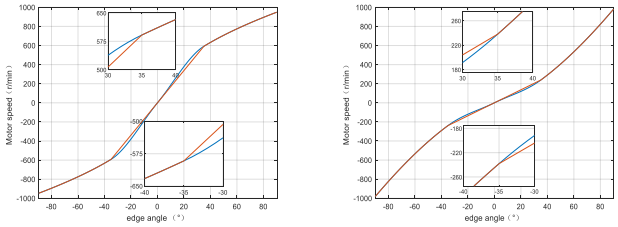
$$\begin{aligned} x &= (\alpha-1)\delta^{\alpha-3} \\ y &= \begin{cases} -(\alpha-1)\delta^{\alpha-2}, 0 \le e \le \delta \\ (\alpha-1)\delta^{\alpha-2}, -\delta \le e \le 0 \end{cases} \\ z &= \delta^{\alpha-1} \end{aligned} \tag{14}$$

The transformed nonlinear function can be expressed as:

$$F = kfal = \begin{cases} k|e|^{\alpha} sign(e), |e| > \delta \\ k[(\alpha-1)\delta^{\alpha-3} \cdot e^3 - \\ (\alpha-1)\delta^{\alpha-2} \cdot e^2 sign(e) + \delta^{\alpha-1} e], |e| \le \delta \end{cases} \tag{15}$$

Where, e as the forward input deviation of the control system, adjust the output of the nonlinear function F by changing k、α、δ three parameters.

The x-axis represents the size of the edge angle, and the y-axis represents the motor speed. The simulation results are shown in Fig.6.



(a) α <1 (b) α >1

Fig.6 *fal* function comparison

The transformed *fal* function transitions according to a smooth trend as a whole, which can effectively solve the problem of the speed change of the motor at the segment point, and make the motor have a lower speed when the edge angle is small. When the edge angle is large, that is, when the motor is running at high speed, either the $\alpha < 1$ exponential function with a slow growth rate or the $\alpha > 1$ exponential function with a faster growth rate can be selected. We can change the parameters α and k to meet the demand for velocity changes in skiing.

4. NEURAL NETWORK PREDICTION BASED ON SPARROW SEARCH ALGORITHM OPTIMIZATION

Due to the slow communication speed between the server, controller, and sensors. When the indoor ski simulator starts, the motor output speed and the skier's position shown on the virtual screen lag relatively. It is found that the simulated skiing effect is not good, so we need to predict the position of the skier in advance. In this section, the attitude data and displacement data measured by the skier after the experience are recorded, then we use the neural network to model and analyze it.

4.1. Sparrow search algorithm

The sparrow search algorithm is inspired by the foraging behavior and anti-predation behavior of sparrows[9]. This search algorithm imitates the foraging process of sparrow populations.

Sparrow populations have two distinct roles in their daily foraging activities, finder, and joiner. The finder is mainly responsible for finding food in the daily population activities, and the joiner obtains food through the information provided by the finder. In addition, sparrows usually use behavioral strategies flexibly. The joiner will forage with the finder, while the vigilant is a part of the members at the edge of the population that forage with the finder. Because they are more vulnerable to other predators, they will try to get closer to a better location to get more food. When one of the birds finds a predator approaching or realizes the danger, it will sound an alarm. The entire population will immediately stop foraging, and fly away collectively to perform anti-predation behavior.

We can suppose that there is a swarm of n sparrows, and put it in a d-dimensional problem variable to be optimized, which can be expressed as:

$$X = \begin{bmatrix} x_{1,1} & x_{1,2} & \cdots & x_{1,d} \\ x_{2,1} & x_{2,2} & \cdots & x_{2,d} \\ \vdots & \vdots & \ddots & \vdots \\ x_{n,1} & x_{n,2} & \cdots & x_{n,d} \end{bmatrix} \tag{16}$$

The fitness value of the entire sparrow population can be expressed as:

$$F_X = \begin{bmatrix} f\left(\begin{bmatrix} x_{1,1} & x_{1,2} & \cdots & x_{1,d} \end{bmatrix}\right) \\ f\left(\begin{bmatrix} x_{2,1} & x_{2,2} & \cdots & x_{2,d} \end{bmatrix}\right) \\ \vdots \\ f\left(\begin{bmatrix} x_{n,1} & x_{n,2} & \cdots & x_{n,d} \end{bmatrix}\right) \end{bmatrix} \tag{17}$$

During each iteration, the finder's location update formula can be expressed as:

$$X_{i,j}^{t+1} = \begin{cases} X_{i,j}^{t} \cdot \exp\left(\dfrac{-i}{\alpha \cdot T}\right) & \mathrm{R}_2 < \mathrm{ST} \\ X_{i,j}^{t} + Q \cdot L & \mathrm{R}_2 \geq \mathrm{ST} \end{cases} \tag{18}$$

Where, t is the current number of iterations, T is the maximum number of iterations of the population, ST indicates a safe value, the value range is $[0.5,1]$. By comparing R_2 with ST, we can judge whether there is danger nearby.

The updated formula of the joiner location is:

$$X_{i,j}^{t+1} = \begin{cases} Q \cdot \exp\left(\dfrac{X_{worst}^{t} - X_{i,j}^{t}}{i^2}\right) & i > n/2 \\ X_{p}^{t+1} + \left|X_{i,j}^{t} - X_{p}^{t+1}\right| \cdot A^{+} \cdot L & otherwise \end{cases} \tag{19}$$

Where X_{worst} represents the global worst position of the sparrow population in the d-dimensional space, X_p represents the optimal location of the sparrow population in the d-dimensional space, when $i > n/2$, indicates that the joiner with poor fitness value has the most there may be no food.

The updated formula for the position of the vigilante is as follows:

$$X_{i,j}^{t+1} = \begin{cases} X_{best}^{t} + \beta \cdot \left|X_{i,j}^{t} - X_{best}^{t}\right| & f_i \neq f_g \\ X_{i,j}^{t} + K\left(\dfrac{\left|X_{i,j}^{t} - X_{worst}^{t}\right|}{(f_i - f_w) + \varepsilon}\right) & f_i = f_g \end{cases} \tag{20}$$

Where X_{best} represents the global optimal position of the sparrow population in the d-dimensional space, K indicates the direction of movement of the sparrow population, f_i indicates the fitness value of the sparrow population, f_g indicates the optimal fitness value of the sparrow population, f_w indicates the worst fitness value of the sparrow population. when $f_i \neq f_g$, indicates that the current sparrow is more likely to be attacked by predators, when $f_i = f_g$, it means that to ensure its safety, the sparrow is constantly adjusting its position to reduce the probability of being attacked by predators.

4.2. Steps to optimize a neural network with the sparrow search algorithm

During the training of the neural network model [10], the sparrow search algorithm can continuously adjust the weights and thresholds of each layer. In this way, the error between the final output results and the expected value is greatly reduced.

The process of optimizing the BP neural network by the sparrow search algorithm is to continuously search for the optimal weights and thresholds of the BP neural network to further improve the convergence velocity of the network and attain the purpose of training.

The steps of the sparrow search algorithm to optimize the BP neural network are [11]:

Step 1: Initialize the relevant parameters of the neural network;

Step 2: Initialize the sparrow population and the ratio of discoverers and joiners. Then define the maximum number of iterations;

Step 3: When the number of iterations is less than the maximum number of iterations, the fitness of the initial population is calculated and the final result is sorted;

Step 4: Renew the location of the sparrow with the highest fitness (discoverer). Renew the location of the sparrow with the lower fitness (joiner). And update the position of the sparrow (vigilante) who feel the danger of the surrounding environment;

Step 5: Obtain the position of the sparrow after the current update. If the position of the current sparrow is better than the old position of the previous iteration, then the update operation is performed, otherwise, the update operation is not performed. Continue the iterative operation according to this step until the position of the sparrow meets the requirements. Finally, the optimal individual and optimal fitness values are obtained from all sparrow populations;

Step 6: Output the obtained global optimal individual and use it as the weight in the BP neural network. Output

The 10th International Symposium on Computational Intelligence and Industrial Applications (ISCIIA2022)
Beijing, China, Sept. 23-Sept. 25, 2022

the got global optimal solution, then use it as the threshold in the BP neural network;

Step 7: In the process of BP neural network training, if the initial set maximum number of iterations is reached or the prediction error is met, stop the calculation and output the current value; else go to step 3 and continue to repeat the above steps.

The process of SSA optimizing the BP neural network is shown in Fig.7.

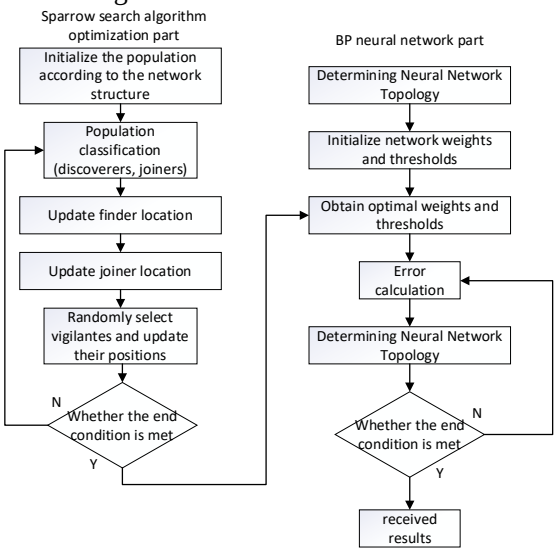
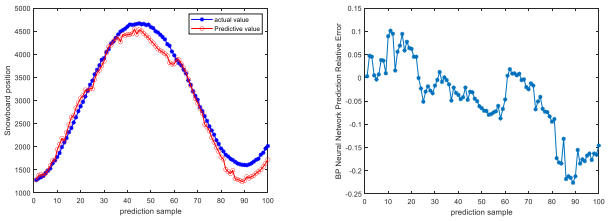


Fig.7 Optimization process

4.3. Analysis of results

After processing collected attitude data and displacement data, the neural network training results are shown in Fig.8. Using the BP neural network to predict the data, it can be seen that there is a large deviation in the experimental results.

Although the number of neurons in the hidden layer of the neural network model is constantly modified, there is still a large error, and the predictability of the data is poor.



(a) Comparative Results (b) forecast relative error

Fig.8 BP neural network experimental results

After using the sparrow search algorithm to optimize the parameters of the BP neural network, simulation results are significantly improved, and the prediction effect is better, as shown in Fig.9 and Fig.10.

When the number of iterations is the 16th, the optimal fitness value is reached. This proves the strong iteration and optimization ability of the sparrow search algorithm, which makes the prediction results of the neural network closer to the real value, and the relative prediction error is controlled by 0.07.

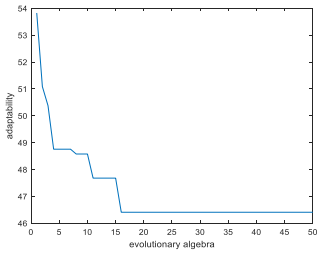
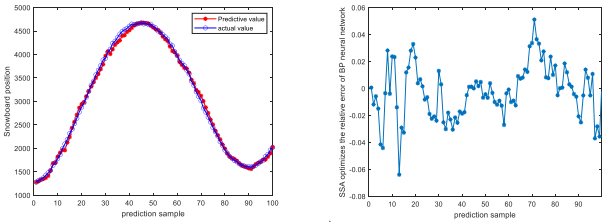


Fig.9 Fitness curve



(a) Comparative Results (b) forecast relative error

Fig.10 Experimental results of sparrow search algorithm optimization of BP neural network

5. CONCLUSIONS

This thesis is based on a self-developed ski simulator for ski training and entertainment and proposes a nonlinear control algorithm for the motor speed of the simulator. Aiming at the lag problem found during the use of the simulator, this thesis uses SSA to optimize the weights and thresholds of the BP neural network. Through the comparison of simulation experiments, it is found that the results are better than the traditional neural network and have a better prediction effect, which makes the simulated skiing experience more realistic.

In future research, a more in-depth study of the simulated ski platform, and the application of SSA in more complex practical applications to better solve engineering problems.

Acknowledgments

This work is supported by Research and Demonstration of Key Technologies in The Construction of the National Scientific Training Base (No.2018YFF0300800).

REFERENCES:

[1] Jianyi Zhang, Bochen Ren. VR ski simulator conceptual design based on user experience [J]. Design, 2020, 33 (1):125-127.

[2] Changjiang Song, Xiaodan Cong, Siwen Sun. Design and Implementation of Visual System of Simulated Ski Machine Based on Unity3D [J].Techniques of Automation and Applications, 2021, 40(3): 158-161.

[3] Zhiwei Wang. Design and Development of Ski Simulator System Based on Virtual Reality[D]. Beijing Jiaotong University, 2017.

[4] Juan Zhou, Shuanghua Wang, Tao Wang. Simulation and Study on Speed Modeling for Alpine Skiing[J]. Computer Integrated Manufacturing Systems, 2015, (9): 226-232.

[5] Thompson B E, Friess W A, Knapp II K N. Aerodynamics of speed skiers[J]. Sports Engineering, 2004(4): 103-112.

[6] Kaps P, Mssner M, Nachbauer W, et al. Pressure Distribution Under a Ski During Carved Turns[C]. Science and skiing. 2001.

[7] Wang Yuhang, Yao Yu, Ma Kemao. Analysis and application of Fal function filter[J]. Electric Machines and Control, 2010, 14(11): 88-91.

[8] Huang Yi, Zhang Wenge. Development of active disturbance rejection controller[J]. Control Theory and Applications, 2002, 19(4): 485-492.

[9] Jiankai Xue, Bo Shen. A novel swarm intelligence optimization approach: sparrow search algorithm[J]. Systems Science & Control Engineering,2020, Vol. 8(1): 22-34.

[10] WU W, WANG J, CHENG M, et al. Convergence analysis of online gradient method for BP neural networks[J]. Neural Networks: The Official Journal of the International Neural Network Society, 2011, 24(1): 91-98.

[11] PAN, JENG-SHYANG, SHAN, JIE, et al. Wind power prediction based on neural network with optimization of adaptive multi-group salp swarm algorithm[J]. Cluster computing, 2021, 24(3): 2083-2098.